Appl Compos Mater (2016) 23:821–837
DOI 10.1007/s10443-016-9487-2

Lightning Strike Ablation Damage Characteristic Analysis for Carbon Fiber/Epoxy Composite Laminate with Fastener

J. J. Yin [1] · S. L. Li [1] · X. L. Yao [2] · F. Chang [1] · L. K. Li [1] · X. H. Zhang [1]

Received: 18 March 2016 / Accepted: 4 April 2016 / Published online: 14 April 2016

Abstract In order to analyze the lightning strike ablation damage characteristic of composite laminate with fastener, based on the energy-balance relationship in lightning strike, mathematical analysis model of ablation damage of composite laminate with fastener was constructed. According to the model, an effective three dimensional thermal-electrical coupling analysis finite element model of composite laminate with fastener suffered from lightning current was established based on ABAQUS, and lightning strike ablation damage characteristic was analyzed. Analytical results reveal that lightning current could conduct through the thickness direction of the laminate due to the existence of metallic fastener, and then distribute to all layers, finally conducted in-the-plane of each layer, conductive ability of different layup orientations depend on potential distribution and in-the-plane electrical conductivity along potential gradient declining direction; different potential boundaries correspond to different potential distribution in each layer, and result in conductive ability of different layup orientations was changed, then caused different lightning strike ablation damage distribution. According to the investigation in this paper, we can recognize the lightning strike ablation damage characteristic of composite laminate with fastener qualitatively.

Keywords Composite laminate with fastener · Lightning strike · Ablation damage characteristic · Thermal-electrical coupling analysis

✉ J. J. Yin
330356322@qq.com

[1] College of Aeronautics and Astronautics Engineering, Airforce Engineering University, No.1, Baling St, Xi'an 710038, China

[2] The State Key Laboratory of Electrical Insulation and Power Equipment, Xi'an Jiao Tong University, No.28, Xianning St, Xi'an 710049, China

1 Introduction

Lightning is a natural phenomenon with high-voltage and high-current, an aircraft may suffer from one lightning strike between each 1000 and 3000 h of flight based on the statistics on airliner, and even once a year especially in regions with much more lightning storms [1, 2]. Lightning strike can cause severe damage to aircraft structure, both metallic and composite, direct effects of lightning strike include burning, melting, resistive heating, magnetic force effects, acoustic shock, arcing and sparking at joints and so on. Compared between traditional metallic structure and composite structure, one of the main drawbacks of composite structure is poor electrical conductivity, about 1/1000 for aluminum alloy, composite structures are easier to suffer from damage under lightning strike direct effects, and the strength and stiffness of composite structure will descend severely.

Damage process of aircraft composite structure subjected to lightning strike is complex and occurs in an extremely short time, which involves interaction of electrical, thermal, mechanical and magnetic phenomena. For the sake of investigating damage behavior of composite structure subjected to lightning strike, investigator had carried out some tests and simulation works with respect to composite lightning strike. Hirano et al. [3] did artificial lightning test on graphite/epoxy laminated composite specimens without lightning protection system, investigated the relationship between damage behavior and lightning strike waveform and peak current, results revealed the damage mode of composite after lightning strike and analyze the form reason. Literature [4–7] presented a coupled thermal-electrical finite element analysis model based on the ABAQUS thermal-electrical analysis module, to elucidate damage behavior caused by a lightning strike based on transient temperature distribution in CFRP when exposed to simulated lightning current. Wang et al. [8] studied the ablation damage characteristic of a carbon fiber/epoxy composite laminate suffered from lightning strike by coupling thermal-electrical-structural analysis and element deletion through ANSYS software. All researches mentioned above are focus on composite laminate, but during the process of aircraft manufacture, metallic fasteners are always used to assemble composite structures, especially in the skin of an aircraft, despite composite-intensive constructions will greatly reduce the number of fasteners by introducing integrated structures. Practically speaking, metallic fasteners on an outer skin are always in danger of a lightning threat because metallic fasteners can create a more attractive path for a lightning leader than a standard composite skin [9]. Feraboli et al. [10] did some simulated lightning strike test researches to investigate damage degree and damage mode of composite specimens with and without fastener, results indicate that under the same peak current, distribution and patterns of lightning strike damage are different when compared between composite laminate with fastener and without fastener, simultaneously, mechanical testing was done to assess the residual tensile and compressive strength, when subjected to lightning strike (peak current 50kA), for composite laminate with fastener, its residual tensile strength improve 2 %, but residual compressive strength descend about 64.2 %; for composite laminate without fastener, its residual tensile strength descend 22 %, and residual compressive strength descend about 31.8 %.

Focus on the difference of lightning strike ablation damage between composite laminate with fastener and without fastener mentioned in literature [10], based on the method of simulation, lightning strike ablation damage characteristic of composite laminate with fastener is investigated in this paper.

2 Mathematical Analysis Model of Lightning Strike Ablation Damage

Composite lightning strike damage can be classified into two main categories: one is the ablation damage due to thermal decomposition of epoxy and sublimation of carbon fiber under the condition of extremely high temperature; another one is the mechanical impact damage due to magnetic force and acoustic pressure [11]. Compared between ablation damage and mechanical impact damage, the former has larger influence on composite load carrying capability. When lightning hit composite structure, lightning current will enter into the structure from lightning attachment point, and generate vast resistive heating due to the poor electrical conductivity of composite, and then ablation damage will occur accompany with temperature rising, simultaneously, heat transfer between high-temperature zone and low-temperature zone in composite will appear also. So that, if just take lightning strike ablation damage into account, the essence of composite lightning strike ablation damage analysis process can be simplified into a problem of nonlinear heat transfer which include inner heat source.

2.1 Heat Transfer Governing Equations

Based on the energy-balance relationship, transient heat transfer governing equations of three-dimensional structure which include inner heat source can be expressed as:

$$\int_S \boldsymbol{q} dS + Q = \int_V \rho c_p \frac{\partial T}{\partial t} dV \tag{1}$$

Where V is any control volume of solid material,with surface area S; $\boldsymbol{q}$ is heat flux per unit area of the body, flowing into the body; T and t are temperature and time respectively; ρ is the density of the material; c_p is specific heat of the material. First term in left side of Eq. (1) represents heat transfer energy between control volume and surroundings, second term Q represents inner heat source generated in the control volume, for the problem of composite lightning strike, this term can represent resistive heating due to lightning current; Term in right side of Eq. (1) represents internal energy increment of the control volume.

Heat conduction is assumed to be governed by Fourier law, heat flux per unit area has the following form:

$$\boldsymbol{q} = -\boldsymbol{K} \frac{\partial T}{\partial x} \tag{2}$$

Where $\boldsymbol{K}$ is thermal conductivity matrix; and x is position. Thermal conductivity $\boldsymbol{K}$ can be fully anisotropic, orthotropic, or isotropic. For orthotropic composite, density of heat flux can be expressed as:

$$\boldsymbol{q} = \begin{bmatrix} q_x \\ q_y \\ q_z \end{bmatrix} = - \begin{bmatrix} k_{xx} & & \\ & k_{yy} & \\ & & k_{zz} \end{bmatrix} \begin{bmatrix} \dfrac{\partial T}{\partial x} \\ \dfrac{\partial T}{\partial y} \\ \dfrac{\partial T}{\partial z} \end{bmatrix} \tag{3}$$

Where x, y and z are the principal axis of the material.

Maximum temperature in local territory of composite laminate may reach as high as 3000 °C because of resistive heating, accompany with temperature rising, composite physical

properties will be changed, so, properties such as thermal conductivity, density and specific heat are all considered as function of temperature. At the same time, during temperature rising, composite epoxy will be decomposed, and metallic fastener will be melted and evaporated, these material status change processes usually are called phase transition, during phase transition, material will consume a lot of energy, which is called latent heat and must be considered. According to literature [12], composite material decomposing latent heat can be added to specific heat, effective specific heat capacity during epoxy decomposition can be expressed by:

$$\begin{gathered} C_p = \quad C_{pb} f_b + \quad C_{pa} f_a + \quad H_s \frac{d\alpha}{dT} \\ f_b = \frac{M_i(1-\alpha)}{M_i(1-\alpha) + M_e\alpha}; \quad f_a = \frac{M_e\alpha}{M_i(1-\alpha) + M_e\alpha} \end{gathered} \tag{4}$$

Where M_e is final mass of composite material; M_i is initial mass of composite material; f_b and f_a are volume fraction of the composite and char material respectively; H_s is decomposition latent heat; α is decomposition degree, which can be expressed by a function of temperature [13]:

$$\alpha = 1-\exp\left[\frac{1}{1-n}\ln\left\{1-(1-n)\int_{t_0}^{t}\frac{A}{\beta}\exp\left(-\frac{E_a}{RT}\right)dT\right\}\right] \tag{5}$$

Where A is pre-exponential factor, E_α is activation energy, R is universal gas constant ($R = 8.314\ J/mol/K$), β is a constant heating rate, n is reaction order.

For metallic material, phase transition latent heat can be added to specific heat too, the relationship between effective specific heat capacity and phase transition latent heat have the following general form [5]:

$$C_p = \frac{H_L}{\Delta T_m} + \frac{C_{ps} + C_{pl}}{2} \tag{6}$$

Where H_L is material latent heat (melting, evaporation), c_{ps} is material specific heat before phase transition critical temperature; c_{pl} is material specific heat after phase transition critical temperature; ΔT_m is temperature range of phase transition.

2.2 Thermal Energy Due to Electrical Current Governing Equations

The electric field in a conducting material is governed by Maxwell's equation of conservation of charge. Assuming steady-state direct current, the equation reduces to [14]:

$$\int_s \mathrm{J}\cdot\mathrm{n}dS = \int_V r_c dV \tag{7}$$

Where V is any control volume whose surface is S, nis the outward normal to S, r_c and is the internal volumetric current source per unit volume, J is the electrical current density (current per unit area), and can be described by Ohm's law:

$$\mathrm{J} = \sigma^E \cdot E = -\sigma^E \cdot \frac{\partial \varphi}{\partial X} \tag{8}$$

In this equation, $E(X)$ is electrical field intensity;ϕ is electrical potential; $\sigma^E(\theta,f^{el})$ is electrical conductivity matrix, θ is temperature, and f^{el} is predefined field variable. The conductivity can be isotropic, orthotropic, or fully anisotropic.

Take Eq. (8) into Eq. (7), the governing conservation of charge equation becomes:

$$\int_v \frac{\partial \delta\varphi}{\partial X}\cdot\sigma^E\cdot\frac{\partial\varphi}{\partial X}\boldsymbol{d}V = \int_S \delta\varphi \boldsymbol{J}\boldsymbol{d}S + \int_v \delta\varphi\cdot r_c \boldsymbol{d}V \tag{9}$$

According to Joule's law, the rate of electrical energy dissipated by current flowing through a conductor can be described as:

$$P_{ec} = \boldsymbol{E}\cdot\boldsymbol{J} = \boldsymbol{E}\cdot\sigma^E\cdot\boldsymbol{E} = \frac{\partial\varphi}{\partial X}\cdot\sigma^E\cdot\frac{\partial\varphi}{\partial X} \tag{10}$$

In a transient analysis an averaged value of P_{ec} is obtained over the time increment, Δt.

$$P_{ec} = \frac{1}{\Delta t}\int_{\Delta t} P_{ec}dt = \boldsymbol{E}\cdot\boldsymbol{\sigma}^E\cdot\boldsymbol{E} - \boldsymbol{E}\cdot\boldsymbol{\sigma}^E\cdot\Delta\boldsymbol{E} + \frac{1}{3}\Delta\boldsymbol{E}\cdot\boldsymbol{\sigma}^E\cdot\Delta\boldsymbol{E} \tag{11}$$

Where E and σ^E are values at time $t+\Delta$t. The amount of this energy released as internal heat is:

$$Q = \eta_v P^v{}_{ec} \tag{12}$$

Where η_v is an energy conversion factor.

2.3 Boundary Conditions

As mentioned before, during lightning strike, maximum temperature in local territory of composite laminate may reach as high as 3000 °C, therefore, there exist two energy exchange models between surface of composite and surroundings, including heat convection and heat radiation. When differential value of temperature between composite and surroundings higher than 400 °C, heat radiation is the main energy exchange model between surface of composite and surroundings. Hence, we adopt the third boundary condition of heat transfer in this paper.

$$q_{em} = B\left(\left(T-T^Z\right)^4 - \left(T^0-T^Z\right)^4\right) \tag{13}$$

Where B is radiation constant (radiation emissivity times Stefan-Boltzmann constant); T^Z is value of absolute zero on temperature scale being used; T is temperature on the surface of the body under consideration; T^0 is temperature of the surroundings.

3 Finite Element Model

Before constructing the finite element model (FEM), we put forward the following assumptions: (1) Lightning strike attachment point wholly locates on the top center of the fastener; (2)

During temperature rising, do not take the physical properties of fastener change into account; (3) There is no clearance exist between composite and fastener, ignore the contact electrical resistance and contact thermal resistance on interface. Based on these assumptions, an effective three dimensional thermal-electrical coupling analysis finite element model of composite laminate with fastener subjected to lightning current is established based on ABAQUS.

Carbon fiber/epoxy composite is HTA/7714 A,with a 16-plies orthotropic layup($[45/0_2/-45/0_3/90]_S$), specimen size is 304.8 mm × 38.1 mm × 2.88 mm, thickness of each ply is 0.18 mm. Metallic fastener locates in the center of the laminate and its diameter is 6.35 mm. During constructing the FEM, refine the mesh around fastener hole of the composite laminate, each layer of the laminate is explicitly discretized by using 3D element. Total number of simulation elements is 37,440 and element type is DC3D8E. Figure 1 shows the FEM of composite laminate with fastener subjected to lightning strike. Material properties of composite and metallic fastener, such as thermal conductivity, electrical conductivity, specific heat and density are given in Table 1 and Table 2.

Heat radiation will occur due to transient heat transmit of the specimen, assuming all surfaces radiate heat, radiation emissivity is 0.9 and environment temperature is 25 °C. Initial temperature of specimen is in accordance with temperature of environment. Taking two potential boundaries into account: one is potential of both ends E = 0 V; another one is potential of side surfaces E = 0 V, the former represents specimen is fixed at both ends, and the later represents all side surfaces of specimen is fixed. Lightning current waveforms T_1/T_2 = 5/27 μs, peak current are 10kA, 30kA, 50kA, 70kA, 100kA and 150kA respectively.

Value of composite epoxy decomposition kinetic parameter in Eq. (5) presented as followed: n = 3.5,A = $5.0*10^{13}$(1/min),E_a = 180($kJ/mol/K$) [4]. Based on Eq. (5), we can get the decomposition degree curves of epoxy under different temperature rising rate (5 °C/min., 10 °C/min., 20 °C/min., 50 °C/min. And 100 °C/min), which is shown in Fig. 2. From Fig. 2, it can be seen that temperature range of epoxy thermal decomposition is about 300 °C ~ 700 °C, latent decomposition heat of epoxy is 4.8 × 10^3 kJ/kg [5], which will be consumed during epoxy thermal decomposition. Final weight M_e after decomposition is about 75.5 % of the initial weight M_i of the sample [6].

Calculating the transient temperature field of the specimen during lightning strike based on the constructed FEM. According to the pyrolysis behavior of composite, when temperature higher than 300 °C, pyrolysis behavior of epoxy will take place, which can be used as damage criteria. Therefore, temperature profile higher than 300 °C of simulation result represent damage region in later analysis.

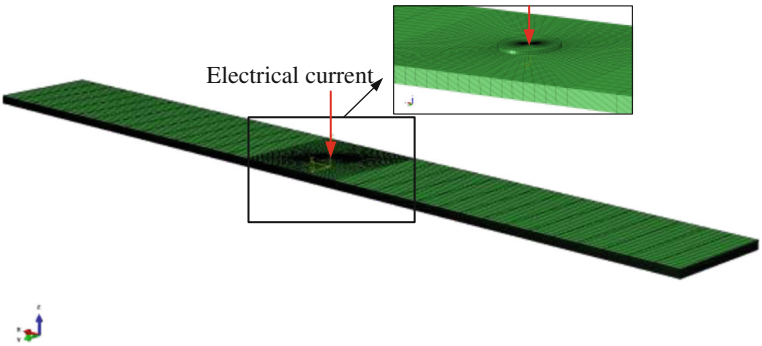

Fig. 1 Finite element model

Table 1 Composite thermal and electrical material properties vs. temperature [5]

Temperature(°C)	Density(kg/m^3)	Specific heat (J/kg°C)	Longitudinal thermal conductivity (W/m°C)	Transverse thermal conductivity (W/m°C)	Longitudinal electrical conductivity (1/Ωm)	Transverse electrical conductivity (1/Ωm)	In depth electrical conductivity (1/Ωm)
25	1520	1065	8	0.67	35,970	1.145	3.876e-3
343	1520	2100	2.608	0.18	35,970	1.145	3.876e-3
500	1100	2100	1.736	0.1	35,970	2000	2000
510	1100	1700	1.736	0.1	35,970	2000	2000
1000	1100	1900	1.736	0.1	35,970	2000	2000
3316	1100	2509	1.736	0.1	35,970	2000	2000
>3316	1100	5875	1.05	1.015	200	200	1e6

Table 2 Material properties of fastener

Density (kg/m^3)	Specific heat (J/kg°C)	Thermal conductivity (W/m°C)	Electrical conductivity (1/Ωm)	Melting temperature (°C)	Melting latent heat (kJ/kg)	Evaporation temperature (°C)	Evaporation latent heat (kJ/kg)
2710	1100	170	3.752×10^6	660	395.7×10^3	2450	$10{,}546 \times 10^3$

4 Results and Discussion

4.1 Distribution of Lightning Strike Ablation Damage

Temperature of colorful region in Fig. 3 is higher than 300 °C, which represent lightning strike ablation damage projected distribution of composite laminate with fastener under different potential boundaries, and peak current is 150kA. It can be seen from Fig. 3a that when potential of both ends $E = 0$ V, ablation damage projection distribute mainly along 0°direction; From Fig. 3b, we can see that when potential of side surfaces $E = 0$ V, ablation damage projection mainly concentrate at center regions of the laminate, and distribute approximately along ±45° and 90°directions.

Lighting strike ablation damage distribution in each layer of composite laminate under different potential boundaries is shown in Fig. 4 and Fig. 5 respectively, colorful areas in Fig. 4 and Fig. 5 represent ablation damage. It can be seen from Fig. 4 that ablation damage in each layer mainly distribute along 0°direction when potential of both ends $E = 0$ V, and ablation damage in 0°layup orientation is much larger than that in other layup orientations; from Fig. 5 we can see that ablation damage exist in ±45°, 90°layup orientations and some 0°layup orientations which border upon ±45° or 90°layup orientations when potential of side surfaces $E = 0$ V, ablation damage in ±45° and 90°layup orientations distribute along its layup orientation, and ablation damage in 0°layup orientations distribute along its nearby layup orientation.

Lightning current could conduct through the thickness direction of the laminate due to the existence of metallic fastener, and then distribute to all layers, finally conduct in-the-plane of each layer. Based on current conduction physical laws, current in conductive medium is

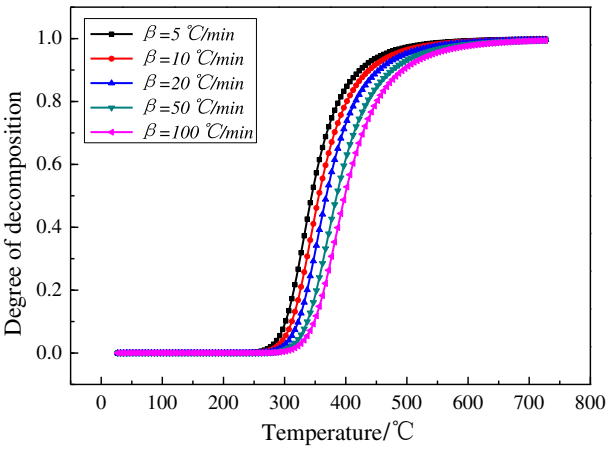

Fig. 2 Decomposition degree curves of resin under diffferent temperature rising rate

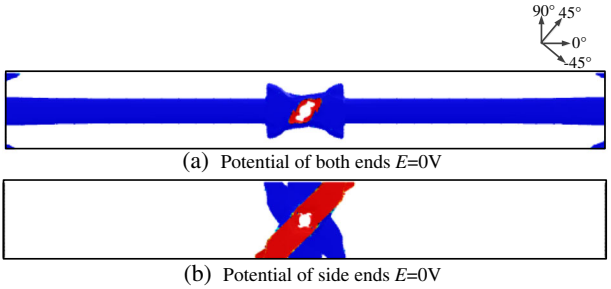

Fig. 3 Damage projected distribution under different potential boundaries

conducted along the direction of potential gradient. Because electrical conductivity of composite is orthotropic, in-the-plane longitudinal electrical conductivity of single layer is much higher than transverse electrical conductivity, therefore, lightning current conduct in single layer of composite must satisfy two basic requirements: first, there must exist potential gradient in-the-plane of layer; second, electrical conductivity along the potential gradient direction is higher in-the-plane of layer.

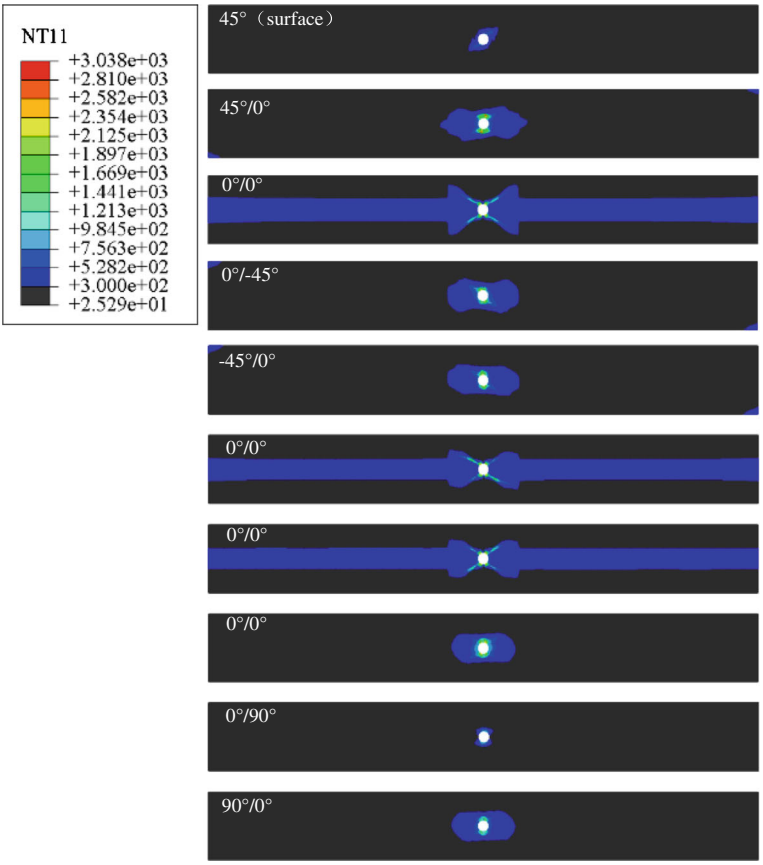

Fig. 4 Damage distribution in each layer when both ends potential $E = 0$ V

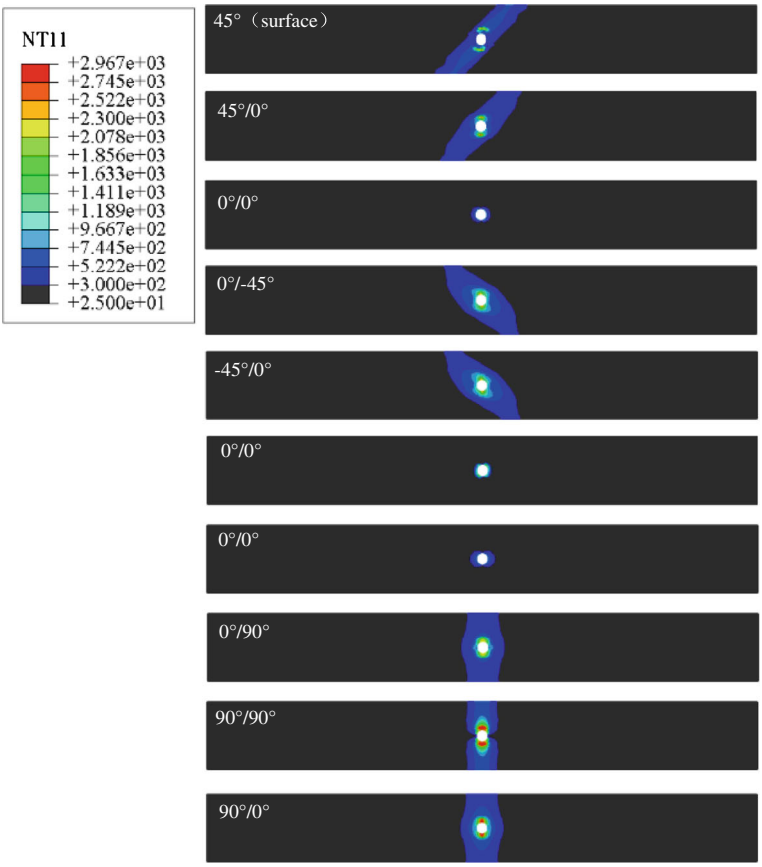

Fig. 5 Damage distribution in each layer when side surfaces potential $E = 0$ V

Figure 6 shows potential distribution in typical layup orientations when laminate both ends potential $E = 0$ V. It can be seen from Fig. 6a that there exist obvious potential gradient in 45° layup orientation along −45°direction, and in the vicinity of the fastener, 45° layup orientation also exist some potential gradient along 45°direction, but after location A, potential keeps almost unchanged. According to the potential distribution and in-the-plane electrical conductivity in 45° layup orientation, we can see that, once lightning current conducted to this layer, 45° layup orientation will conduct lightning current in the vicinity of the fastener along 45°direction. Figure 7 shows the amount of electrical current per unit area in 45° layup orientation. From Fig. 7, we can see that current distribution simulation result correspond to analysis above, because there exist no obvious potential gradient after location A, when lightning current conduct to location A, it cannot be conducted to the boundary along 45°direction, and it will conduct along other direction, such as transverse direction and thickness direction, which have larger potential gradient, under this condition, lightning current conduction will be severely impeded. Above all, when potential of both ends $E = 0$ V, 45° layup orientation will conduct lightning current in the vicinity of the fastener along 45°direction, but due to its potential distribution, its lightning current conductive ability is confined. Adopting the same analysis method above, we can get the lightning current conductive ability

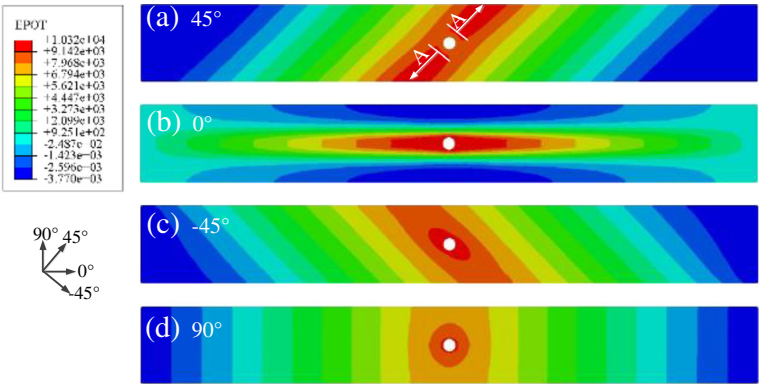

Fig. 6 Potential distribution in typical layup orientation when both ends potential $E = 0$ V

of 0°, −45°and 90°layup orientations from Fig. 6b, c and d respectively: (1) For −45°and 90°layup orientations, they have the same lightning current conductive ability with 45° layup orientation. Once lightning current conducted to these layers, lightning current just be conducted in the vicinity of the fastener and along the layup orientation, but cannot be conducted to the boundary; (2) For 0°layup orientation, based on its potential distribution and in-the-plane electrical conductivity, once lightning current conducted to this layer, it will conduct lightning current along 0°direction, the largest discrimination between 0°layup orientation and other layup orientations is lightning current could be conducted to the boundary of 0°layup orientation along 0°direction, and it can form a complete current conduction channel. Hence, 0°layup orientation have super current conductive ability when compared to other layup orientations under the condition of both ends potential $E = 0$ V.

Figure 8 shows potential distribution in typical layup orientations when laminate side surfaces potential $E = 0$ V. It can be seen from Fig. 8 that potential in each typical layer approximately decline from center to all around gradually. Once lightning current conduct to each layer through fastener, it will be conducted away along the higher electrical conductivity direction in-the-plane of each layer. From Fig. 8 a, c and d, we can see that lightning current in $\pm 45^{\circ}$ and 90°layup orientations will be conducted away along respective layup orientation, and also could be conducted to the boundary, form a complete current conduction channel. From Fig. 8b, lightning current in 0°layup orientation will be conducted in the vicinity of the fastener and along 0°direction, but we can see from Fig. 8b that there exist no potential gradient in regions after location B, when lightning current conduct to location B, it cannot be conducted to the boundary along 0°direction, and it will conduct along other direction, such as transverse

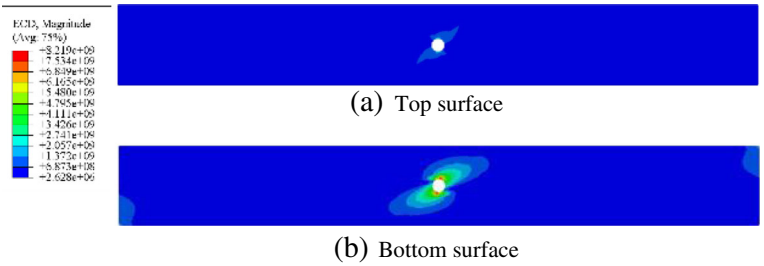

Fig. 7 Electrical current per unit area distribution

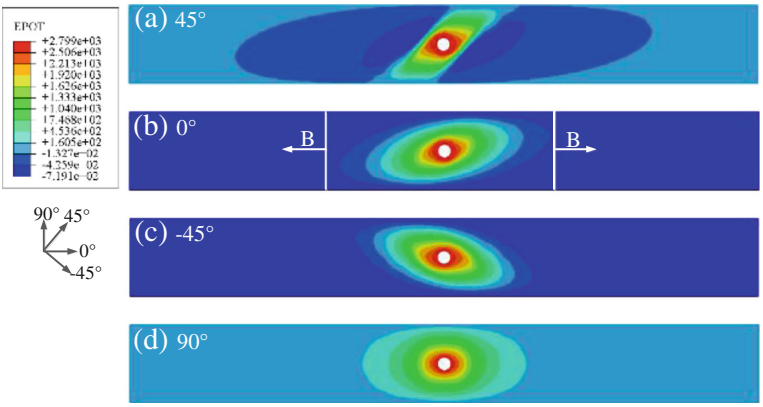

Fig. 8 Potential distribution in typical layup orientation when side surfaces potential $E = 0$ V

direction and thickness direction, which have larger potential gradient, under this condition, lightning current conduction will be severely impeded. Above all, when potential of side surfaces $E = 0$ V, 0° layup orientation will conduct lightning current in the vicinity of the fastener along 0°direction, but due to its potential distribution, its lightning current conductive ability is confined.

According to the analysis above, sketch map of lightning current conductive path under different potential boundaries is shown in Fig. 9. Red long dash lines in Fig. 9 represent main lightning current conductive path, most of lightning current conducted away through these paths; Black short dash lines in Fig. 9 represent minor lightning current conductive paths, they cannot conducted away much more lightning current. Left side in Fig. 9 gives lightning current conductive path when potential of both ends $E = 0$ V, under this potential boundary condition, lightning current mainly conduct in-the-plane of all 0°layup orientations. Right side in Fig. 9 gives lightning current conductive path when potential of side surfaces $E = 0$ V, under this potential boundary condition, lightning current mainly conduct in-the-plane of ±45° and 90°layup orientations.

Based on lightning current conductive path analysis in typical layup orientations under different potential boundaries, we can explain the ablation damage distribution under different potential boundaries reasonably. When potential of both ends $E = 0$ V, lightning current mainly conduct in 0°layup orientations, under the act of resistive heating, temperature in these layers will rising promptly, and then ablation damage will occur due to epoxy decomposition, at the

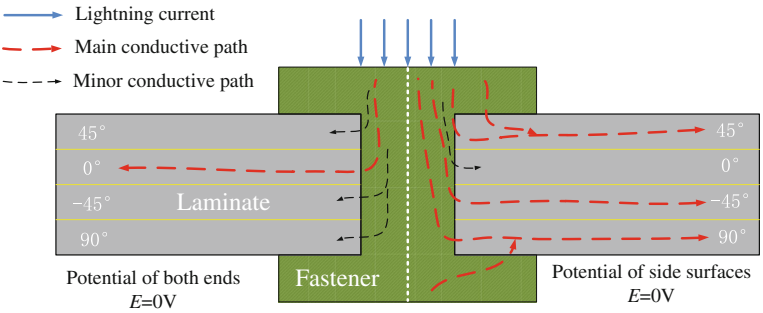

Fig. 9 Sketch map of lightning current conductive path under different potential boundaries

same time, other layup orientations which border upon 0°layup orientations will also appear ablation damage because of heat transfer. Similarly, when potential of side surfaces E = 0 V, lightning current conduct in ±45° and 90°layup orientations mainly, under the act of resistive heating, temperature in these layers will rising promptly, and then ablation damage will occur due to epoxy decomposition, 0°layup orientations which border upon ±45° and 90°layup orientations will also appear ablation damage because of heat transfer.

Figure 10 shows damage images of test specimen from literature [10], white ellipse in Fig. 10a represents lightning strike ablation damage region for composite laminate without fastener, it can be seen from Fig. 10a that lightning strike ablation damage in composite laminate without fastener was confined within shallower regions near the lightning strike attachment point. From Fig. 4 and Fig. 5 we can see that for composite laminate with fastener, ablation damage exists in each layer, even the bottom layer. According to Fig. 10b, there exist wide-ranging delamination damage among layers, there also exist fiber breakage damage, but this kind of damage is mainly confined in the vicinity of the fastener. Based on ablation damage simulation results and test damage results for composite with fastener, we can draw the conclusion that lightning ablation damage of composite with fastener will mainly result in delamination damage for composite laminate, there is no obvious concept of ablation damage depth like lightning ablation damage of composite without fastener. This is the biggest difference between composite with fastener and without fastener. According to the ablation damage characteristic of composite with fastener got in this paper, and combining residual strength test results for composite with fastener in literature [10], we can explain its residual strength change reasonably. Based on the test data in literature [10], under the same peak current (50kA), tensile residual strength improved 2 %, but for compression residual strength, it declined about 64.2 %. Wide-ranging ablation damage among layers will descend the inter-laminar strength, even result in delamination damage, all these damage will influence the compression residual strength severely. However, ablation damage do not cause severe fiber breakage damage, fiber still can bear considerable tensile load, so, tensile residual strength changes little.

4.2 Lightning Ablation Damage Degree

Figure 11 shows ablation damage projected area under different temperature profiles, and lightning peak current is 150kA. According to epoxy decomposition curves in Fig. 2,

(a) Composite laminate without fastener

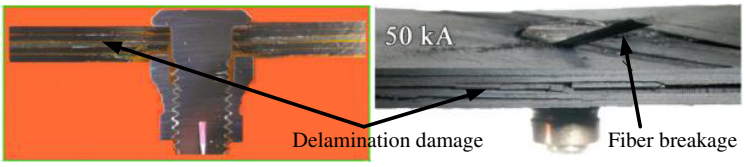

(b) Composite laminate with fastener

Fig. 10 Damage images of test specimen from literature [10]

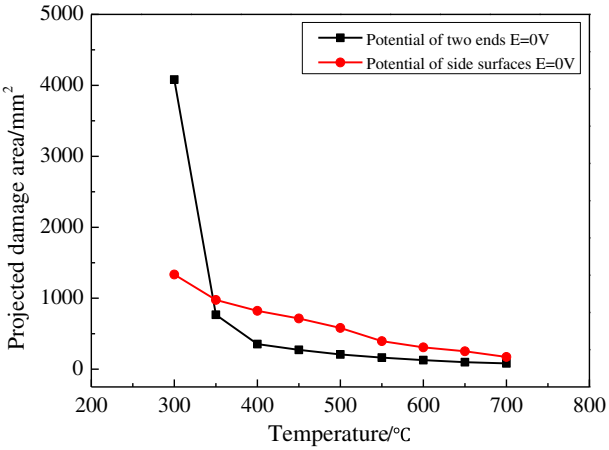

Fig. 11 Damage degree under different temperature

decomposition temperature range of epoxy is 300 °C ~ 700 °C, hence, ablation damage projected area under different temperatures in Fig. 11 could represent lightning ablation damage serious degree. It can be seen from Fig. 11 that when temperature lower than 340 °C, ablation damage projected area of potential of both ends $E = 0$ V is larger than that of potential of side surfaces $E = 0$ V; however, when temperature higher than 340 °C, ablation damage projected area of potential of side surfaces $E = 0$ V is larger. Results in Fig. 11 indicate that total epoxy decomposition regions is larger when potential of both ends $E = 0$ V, but regions of epoxy with high decomposition degree (decomposition degree > 0.2) is smaller than that of potential of side surfaces $E = 0$ V, this means that under the same peak current, lightning ablation damage serious degree of potential of both ends $E = 0$ V is lower although it has larger epoxy decomposition regions.

Figure 12 shows ablation damage projected area under different peak currents and its fitting curves. From Fig. 12, we can see that when potential of both ends $E = 0$ V, increasing rate of ablation damage projected area increase gradually accompany with the increase of peak current. When potential of side surfaces $E = 0$ V, increasing rate of ablation damage projected area changes smoothly, but it also can be divided into three stages: when the peak current lower than 50kA, ablation damage projected area increases slowly; when the peak current locates in 50kA to 125kA, increasing rate of ablation damage projected area is higher than the

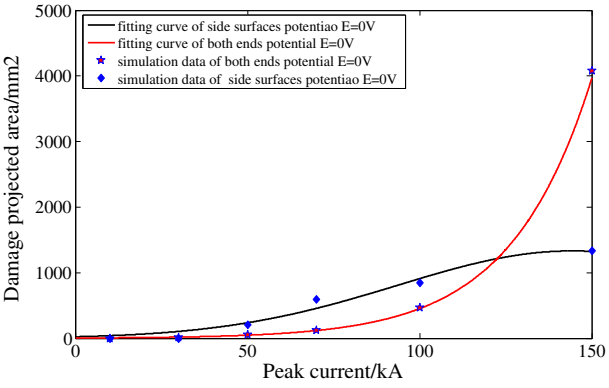

Fig. 12 Damage projected area under different peak current

former stage; when the peak current is higher than 125kA, ablation damage projected area increases slowly again. Compared ablation damage projected area between potential of both ends $E = 0$ V and potential of side surfaces $E = 0$ V, when peak current lower than 125kA, the former ablation damage projected area is smaller than that of the later under the same peak current; on the contrary, when the peak current is higher than 125kA, the former ablation damage projected area is larger under the same peak current, and accompany with the increase of peak current, differential value of ablation damage projected area between them increase promptly.

According to lightning current conductive path analysis in chapter 3.1, when potential of both ends $E = 0$ V, lightning current mainly conduct in 0°layup orientations, and there exist ten layers of 0°layup orientation in FEM; when potential of side surfaces $E = 0$ V, lightning current mainly conduct in $\pm 45^{\circ}$ and 90°layup orientations, and there exist six layers in FEM. Based on potential gradient direction and in-the-plane electrical conductivity of each layer, mainly lightning current conductive regions in typical layup orientations under different potential boundaries is shown in Fig. 13. We can see from Fig. 13 that lightning current conductive territory in 0°layup orientation is larger than other layup orientations.

Combining the number of conductive layers and lightning current conductive regions per layer under different potential boundaries, we can explain the change trend of ablation damage projected area in Fig. 11 reasonably. When total energy of lightning strike is fixed (with the same peak current and waveforms), compared total lightning current conductive regions (conductive regions in per layer times number of layer) between potential of both ends $E = 0$ V and potential of side surfaces $E = 0$ V, the former is larger than the later, therefore, once ablation damage appear, especially the total energy is higher (150kA), ablation damage projected area of former will larger due to the larger lightning current conductive regions, however, under the condition of the former potential boundaries, its energy of per unit area is lower than that of the later, so, ablation damage regions due to epoxy with high decomposition degree is smaller.

Based on the relationship between total energy of lightning and energy of per unit area in lightning current conductive regions under different potential boundaries, we can explain the change trend of ablation damage projected area in Fig. 12 reasonably also. When potential of both ends $E = 0$ V, it has larger lightning current conductive regions, when peak current is less than some value, energy of per unit area in lightning current conductive regions is limited, and cannot cause abroad ablation damage, but when peak current is higher than a critical value, energy of per unit area in lightning current conductive regions is enough to cause abroad ablation damage, therefore, increasing rate of ablation damage projected area has a significant

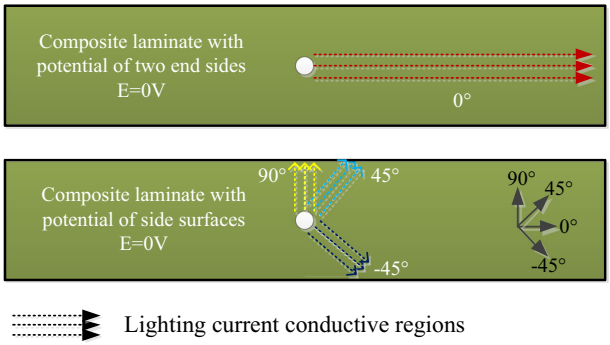

Fig. 13 Lightning current conductive territory under different potential boundaries

transition when peak current is 100kA. When potential of side surfaces $E = 0$ V, its lightning current conductive regions is limited, result in that its energy of per unit area in lightning current conductive regions is higher than that of potential of both ends $E = 0$ V, even though with low peak current, so, under the same current which is less than 125kA, its ablation damage projected area is higher than that of potential of both ends $E = 0$ V, but when the peak current higher than 125kA, because of its lightning current conductive regions is limited and the in-the-plane transverse electrical conductivity is extremely low, so, the ablation damage projected area will not increase, energy of lightning will consumed by deepening the epoxy decomposition degree in exist ablation damage regions.

5 Conclusions

Based on the energy-balance relationship in lightning strike, mathematical analysis model of ablation damage of composite laminate with fastener was constructed in this paper. According to the model, an effective three dimensional thermal-electrical coupling analysis FEM of composite laminate with fastener subjected to lightning current had been established based on ABAQUS, and lightning strike ablation damage characteristic of composite laminate with fastener was analyzed. Analytical results reveal that lightning current could pass through the thickness direction of the laminate due to the existence of metallic fastener, then distribute to all layers, and finally conducted in-the-plane of each layer, conductive ability of different layup orientations is dependent on the potential distribution and in-the-plane electrical conductivity along the potential gradient declining direction, lightning ablation damage exist in both layers which conduct lightning current and layers border upon lightning current conductive layers. Lightning ablation damage in each layer will mainly result in delamination damage of composite, and there is no obvious concept of ablation damage depth like lightning ablation damage of composite without fastener. Ablation damage degree is dependent on total lightning current conductive regions of all the conductive layers, under the same peak current, the larger total lightning current conductive regions, the lower ablation damage degree. For the model constructed in this paper, when the potential of both ends $E = 0$ V, lightning current will mainly conduct in 0° layup orientations, and ablation damage will occurs in these layers, at the same time, other layup orientations which border upon 0° layup orientations will exist ablation damage due to heat transfer; when the potential of side surfaces $E = 0$ V, $\pm 45^{\circ}$ and 90° layup orientations will mainly conduct lightning current, and ablation damage will occurs in these layers, all the same, 0° layup orientations which border upon these layers will exist ablation damage due to heat transfer. Compared between potential of both ends $E = 0$ V and potential of side surfaces $E = 0$ V, the former total lightning current conductive territory is larger than the later, so, its ablation damage degree is lower than the later under the same peak current.

Acknowledgments This study is supported by the National Natural Science Foundation (No: 51477132).

References

1. Uman M.A., Rakov V.A.: The interaction of lightning with airborne vehicles. Prog. Aerosp. Sci. **39**, 61–81 (2003)

2. Gagne M., Therriault D.: Lightning strike protection of composites. Prog. Aerosp. Sci. **64**, 1–16 (2014)
3. Hirano Y., Katsumata S., Iwahori Y.: Artificial lightning on graphite/epoxy composite laminate. Compos. Part A. **41**, 1461–1470 (2010)
4. Ogasawara T., Hirano Y., Yoshimura A.: Coupled thermal–electrical analysis for carbon fiber/epoxy composites exposed to simulated lightning current. Compos. Part A. **41**, 973–983 (2010)
5. Abdelal G., Murphy A.: Nonlinear numerical modeling of lightning strike effect on composite panels with temperature dependent material properties. Compos. Struct. **109**, 268–278 (2014)
6. Dong Q., Guo Y.L., Sun X.C.: Coupled electrical-thermal-pyrolytic analysis of carbon fiber/epoxy composites subjected to lightning strike. Polymer. **56**, 385–394 (2015)
7. Munoz R., Delgado S., Gonzalez C.: Modeling lightning impact thermo-mechanical damage on composite materials. Appl. Compos. Mater. **21**, 149–164 (2014)
8. Wang F.S., Ding N., Liu Z.Q.: Ablation damage characteristic and residual strength prediction of carbon fiber/epoxy composite suffered from lightning strike. Compos. Struct. **117**, 222–233 (2014)
9. Kawakami, H.: Lightning strike induced damage mechanisms of carbon fiber composites. Doctoral Thesis of University of Washington (2007).
10. Feraboli P., Miller M.: Damage resistance and tolerance of carbon/epoxy composite coupons subjected to simulated lightning strike. Compos. Part A. **40**, 954–967 (2009)
11. Chemartin, L., Lalande, P., Peyrou, B.: Direct effects of lightning on aircraft structure: analysis of the thermal, electrical and mechanical constraints. J. Aerospace Lab. (5), 1–15 (2012)
12. Bai Y., Keller T., Vallee T.: Modeling of Thermo-Physical Properties and Thermal Responses for FRP Composites in Fire. Asia-Pacific Conference on FRP in Structures, APFIS (2007)
13. Lee J.H., Kim K.S., Kim H.: Determination of kinetic parameters during the thermal decomposition of epoxy/carbon fiber composite material. Korean J. Chem. Eng. **30**, 955–962 (2013)
14. ABAQUS Users' Manual, version 6.14: 2.12.1 Coupled thermal-electrical analysis. ABAQUS, Inc. (2014)